Geof. Int. Vol. 25-3, 1986, pp. 423–442

TWO DIMENSIONAL FINITE DIFFERENCE SIMULATION OF MAGNETOTELLURIC AND MAGNETIC VARIATION SOUNDINGS WHEN THE SOURCE FIELD IS CONSIDERED

L. J. ALVAREZ*

(Received: July 25, 1984)
(Accepted: February 19, 1986)

RESUMEN

Se describe un algoritmo de diferencias finitas en dos dimensiones para simular sondeos magnetotelúricos (MT) y de variaciones magnéticas (VM). Este algoritmo fue desarrollado con el objeto de comparar estudios de resistividad aparente realizados con uno y otro método. Se considera una fuente de campo con geometría finita. Se presentan resultados de una simulación de este tipo de sondeos en Islandia para ilustrar las aplicaciones de este algoritmo.

ABSTRACT

We describe a two dimensional finite difference algorithm for the simulation of magneto-telluric (MT) and magnetic variation (MV) soundings. The algorithm was developed in order to compare apparent resistivity studies performed with these two methods. A source field with a finite geometry is considered. We illustrate an application of our algorithm through a simulation of this kind of soundings in Iceland.

INTRODUCTION

In the interpretation of magnetotelluric (MT) and magnetic variation (MV) soundings, one often faces the problem of having both lateral heterogeneities of conductivity and finite geometries of the source field. When simulating MV observations, the plane wave approach is inadequate since the gradient of the horizontal magnetic field is always null away from lateral inhomogeneities. In order to properly simulate MT and MV observations when lateral inhomogeneities are present, we have developed a finite difference algorithm that solves the diffusion equation derived from Maxwell's equations and accounts for both the lateral discontinuities in conductivity

* *Department of Geological Sciences, Brown University, Providence, R. I. 02912, U. S. A.*

* *Now at Departamento de Física, Universidad Autónoma Metropolitana, Apdo. Postal 55-534, CP 09340, México, D. F. (Iztapalapa) MEXICO.*

and the finite geometry of the source. The solution is restricted to two dimensions and to a current source flowing parallel to the strike of the geolectric discontinuities. For simulating the source effect itself, we have based our formulation on the previous work of Price (1962). To investigate the effect of lateral heterogeneities we utilized a finite difference approach (Jones and Pascoe, 1971) which, while not unlike the approach of Hibbs and Jones (1973), accounts for the criticisms of Williamson *et al.* (1974).

The motivation of this study is in the first place the need to have a simulator of MV measurements in order to better understand the field data. Besides, there is the intuitive idea that MV soundings are less sensitive to shallow conductive bodies than the MT ones (Kuckes, 1973a). With the help of our algorithm questions like this can be clarified.

MATHEMATICAL FORMULATION

We consider a plane n-layered earth with electrical properties as shown in Fig. 1. Within each layer, Maxwell's equations hold and are given in the MKS system, by (see for example Ramo, Whinnery and Van Duzer, 1965)

$$\nabla \cdot \vec{E} = 0 \tag{1}$$

$$\nabla \cdot \vec{H} = 0 \tag{2}$$

$$\nabla \cdot \vec{E} = -i\omega\mu H \tag{3}$$

$$\nabla \times \vec{H} = \sigma\vec{E} \tag{4}$$

Where $\vec{E}$ and $\vec{H}$ are the electric and magnetic fields respectively, ω is their frequency and σ and μ are the conductivity and permeability of the medium respectively. Here we have assumed an implicit time dependence of the form exp ($i\omega t$) and that the displacement currents are negligible in comparison with the conduction currents for the conductivities and frequencies considered, ($\omega\epsilon << \sigma$).

From equation 3 we can write the diffusion equation as

$$\nabla^2\vec{E} = i\omega\mu\sigma\vec{E} \tag{5}$$

Assuming a constant source field in the y direction we can rewrite equation 5 as

$$\frac{\partial^2 E_y}{\partial x^2} + \frac{\partial^2 E_y}{\partial z^2} = i\omega\mu\sigma E_y \tag{6}$$

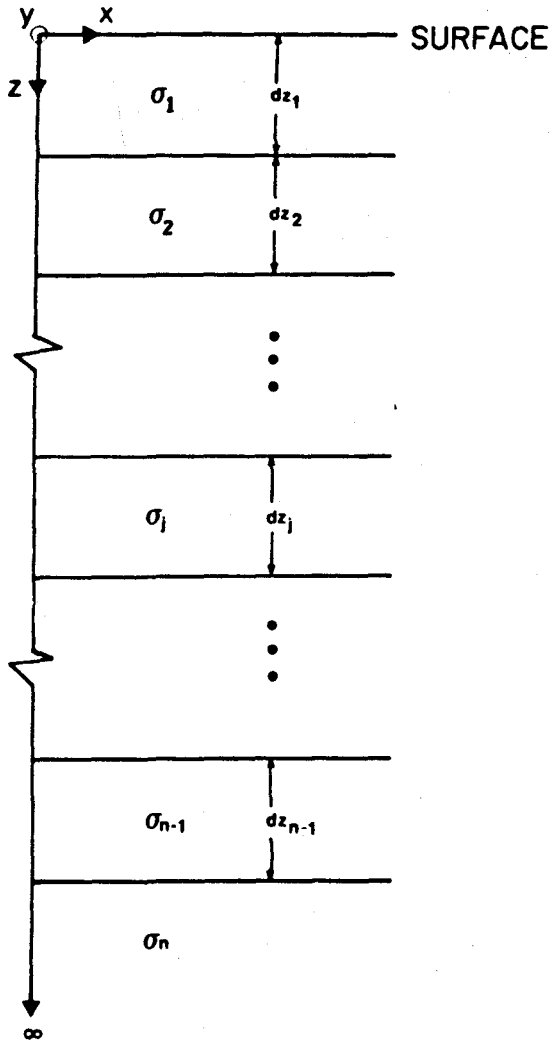

$$R = \frac{Z_o - Z'}{Z_o + Z'}$$

$$Z_j = \frac{i\omega\mu}{(k^2 + i\omega\mu\sigma_j)^{1/2}}$$

Fig. 1. N-layered one - dimensional earth for use in the magnetotelluric formulation.

The solution to equation 6 can be found using the method of separation of variables to obtain for the J-th layer

$$E_y^j(x, z, k) = C_0 [A_j e^{\gamma_j z} + B_j e^{-\gamma_j z}] \cos(kx) \tag{7}$$

where

$$\gamma_j = (k^2 + i\omega\mu\sigma_j)^{1/2} \tag{8}$$

and

$$z_j < z < z_{j+1}\,, \tag{9}$$

σ_j is the conductivity of the j-th layer, C_0 is a parameter that depends on the source, k is the spatial wave number and A_j and B_j are constants to be determined.

Using equation 3 we can calculate the magnetic fields associated with the electric field in each layer as

$$H_x^j = \frac{1}{i\omega\mu} \gamma_j [A_j e^{\gamma_j z} - B_j^{-\gamma_j z}] C_0 \cos(kx) \tag{10}$$

and

$$H_z^j = -\frac{k}{\omega\mu} [A_j e^{\gamma_j z} + B_j e^{-\gamma_j z}] C_0 \sin(kx) \tag{11}$$

Using equations 7 and 10 we define the surface impedance at the j-th interface as

$$Z^j = E_y^j / H_x^j \tag{12}$$

and the characteristic impedance of the j-th medium as

$$Z_j = \frac{i\omega\mu}{\gamma_j} = \frac{i\omega\mu}{\sqrt{k^2 + i\omega\mu\sigma_j}} \tag{13}$$

Invoking the continuity boundary conditions of the tangential electric and magnetic fields along the top of the j-th interface we can develop a recursive formula for the surface impedance given by (Hermance, 1978)

$$Z^{j-1} = Z_{j-1} \frac{Z^j + Z_{j-1} \tanh(\gamma_{j-1} dz_{j-1})}{Z^j \tanh(\gamma_{j-1} dz_{j-1}) + Z_{j-1}} \tag{14}$$

This expression is then used to calculate the surface impedance at the earth's surface, Z^1, and the reflection coefficient due to the stratified structure given by

$$R = (Z_0 - Z^1)/(Z_0 + Z^1) \tag{15}$$

where Z_0 is the characteristic impedance of the air.

We shall consider the effect of the electromagnetic field due to a line current. The term C_0 in equation 7 accounts for the geometry of the source and has to be determined explicitly. Let us consider a homogeneous space of conductivity $\sigma = 0$. The horizontal component of the magnetic field, Hx, is calculated using Ampere's law for a line current of magnitude I_0 as

$$H_x = -\left(\frac{I_0}{2\P}\right) \frac{z - z_0}{(z - z_0)^2 + x^2} \tag{16}$$

where $(0, z_0)$ is the position of the line current and the field is given at the point (x, z) as shown in figure 2.

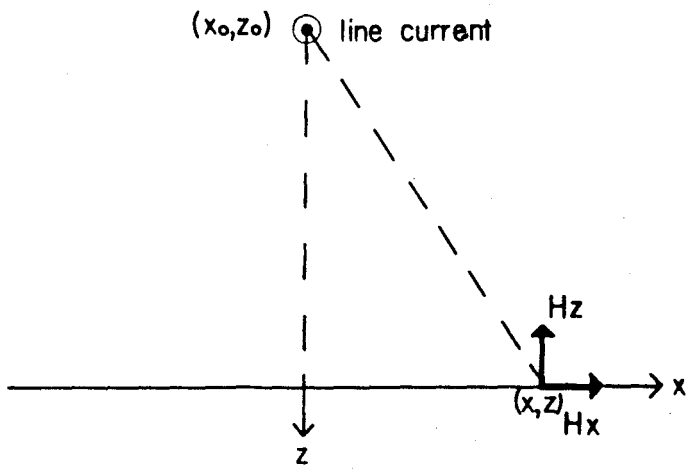

Fig. 2. Magnetic field due to a line current. The field is given by Ampere's law.

From equation 10 we can express the horizontal component of the magnetic field as

$$H_x = \frac{1}{i\omega\mu} k C_0 e^{-kz}\cos(kx) \tag{17}$$

The general solution for Hx is obtained by summing all possible solutions of the form (17) over the allowable range of k, $0 < k < \infty$. Then

$$H_x = \frac{1}{i\omega\mu} \int_0^\infty k e^{-kz} \cos(kx)\, C_0 dk \tag{18}$$

$$= -\frac{I_0}{2\P} (z - z_0)/((z - z_0)^2 + x^2)$$

Using the inverse Fourier transform we notice that

$$-\frac{I_0}{2\P} \frac{(z - z_0)}{(z - z_0)^2 + x^2} = \frac{I_0}{2\P} \int_0^\infty e^{-k(z-z_0)}\cos(kx)\, dk \tag{19}$$

Thus we can use the last two expressions to solve for C_0, ie.:

$$C_0 = -\frac{i\omega\mu\ I_0}{2\P k} e^{kz} \tag{20}$$

FINITE DIFFERENCE SIMULATION

In order to solve equation 6 numerically we superpose a rectangular non-uniform mesh to the model. The mesh is defined by a set of orthogonal straight lines whose interceptions define a set of nodes. Each node has associated the electrical conductivity of the south-eastern rectangle next to it.

The spacings between nodes $dx_j = x_j - x_{j-1}$ and $dz_k = z_k - z_{k-1}$ in the x and z axes respectively are adjustable to the specific requirements of the model. The boundary conditions at the extremes of the model and at the top nodal plane must be defined explicitly. The three planes where the electric field is calculated are shown in figure 3. Along the top nodal plane we use the analytical values of the electric field

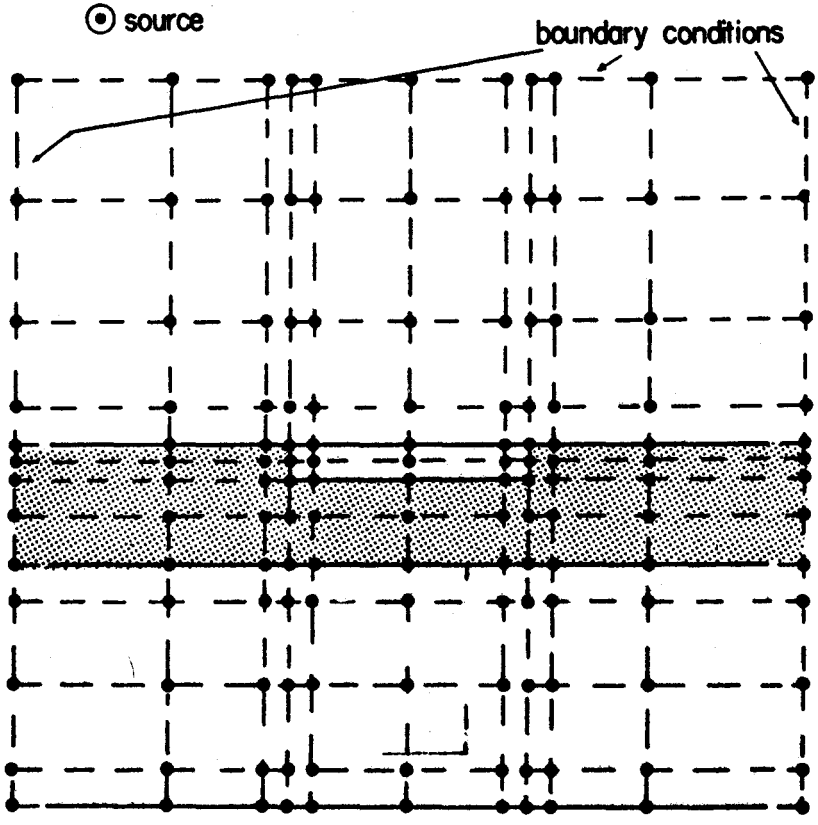

Fig. 3. Nodal mesh superposed to the model for fimite difference calculations. Boundary conditions must be given explicitly at the shown nodal lines.

and assume that the secondary field produced by reflections on embedded heterogeneities or non-horizontal contacts attenuates, and the electric field can be described by the response of a horizontally homogeneous layered medium. Therefore we use equation 15 to describe the reflection coefficient and this, in turn, to express the electric field at the top nodal plane as

$$E(\text{total} = (1 - R)\, E(\text{source}) \qquad (21)$$

where E(source) is obtained from equations 7 and 20 as

$$E(\text{source}) = -\frac{i\omega\mu\ I_0}{2\P k}\ e^{-k(z-z_0)}\cos(kx) \tag{22}$$

In order to calculate the electric field at the extreme vertical nodal planes we express the electric field within each layer in the general form

$$E_T^j = A_j e^{\gamma_j z} + B_j e^{-\gamma_j z} \tag{23}$$

Solving for the constants A_j and B_j in terms of the characteristic impedance of that layer and the surface impedance at its bottom, we find the recursion relations

$$E_T^j\ \Big|_{j+1} = A_j e^{\gamma_j dz_j} + B_j e^{-\gamma_j dz_j} \tag{24}$$

$$A_{j+1} = \frac{Z^{j+1} - Z_{j+1}}{2Z^{j+1}}\ E_T^j\ \Big|_{j+1} \tag{25}$$

$$B_{j+1} = \frac{Z^{j+1} + Z_{j+1}}{2Z^{j+1}}\ E_T^j\ \Big|_{j+1} \tag{26}$$

where dz_j are the vertical spacings between horizontal planes. Thus, given the source field and the reflection coefficient, we use equations 24 to 26 to explicitly calculate

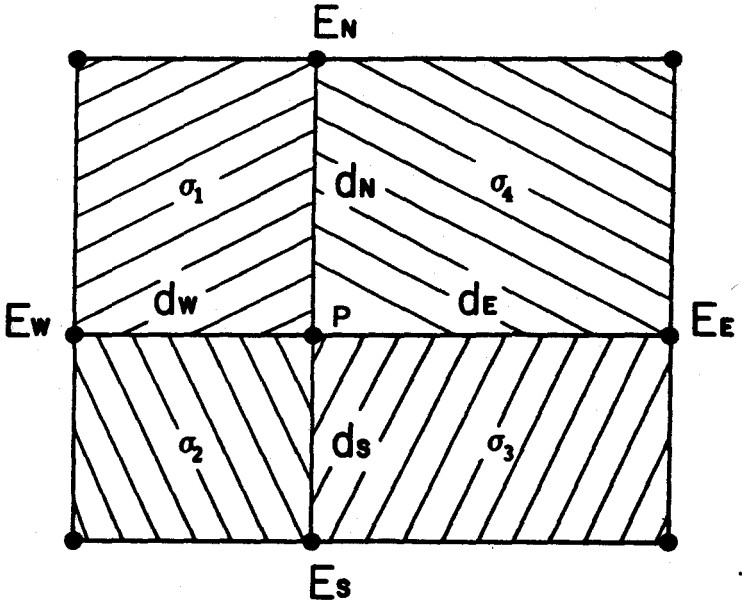

Fig. 4. General situation showing a node with adjacent media with different dimensions and electrical conductivities.

the electric field at the vertical nodal planes at the extremes of the model, starting at the uppermost node and propagating the calculations downward until reaching the lowermost node. At the bottom of the model the boundary condition is that the surface impedance at the last nodal plane is equal to the characteristic impedance of the medium below ($Z^n = Z_{n+1}$). These boundary conditions along with a five point finite difference operator are used to solve the diffusion equation. In the general situation depicted in figure 4, where the four regions around the nodal point P have different conductivities, the following equation has to be solved

$$\begin{aligned} E_p &- (d_W + d_E)(E_N - E_p)/2d_N\beta_e \\ &- (d_W + d_E)(E_S - E_p)/2d_S\beta_e \\ &- (d_N + d_S)(E_W - E_p)/2d_W\beta_e \\ &- (d_N + d_S)(E_E - E_p)/2d_E\beta_e = 0 \end{aligned} \tag{27}$$

where the function E represents the electric field at each of the five points and d_E, d_W, d_N, and d_S are the spacings between the nodal point P and the nodal points to the east, west, north and south respectively and β_e, the electric polarization parameter, is given by

$$\beta_e = i\omega\mu(\sigma_1 d_N d_W + \sigma_2 d_W d_S + \sigma_3 d_S d_E + \sigma_4 d_N d_E)/4 \tag{28}$$

σ_1, etc., being the conductivities associated to the rectangular regions as shown in the figure. This operator was developed by Hermance (1976) and accounts for the criticisms of Williamson *et al.* (1974) regarding the finite difference scheme of Jones and Pascoe (1971). Our algorithm allows for irregular spacings between nodes as well as for sharp conductivity changes across interfaces in the vicinity of each node. Equivalent operators have been developed by Brewitt-Taylor and Weaver (1976) and Praus (1976).

Care most be taken in the choice of the mesh size in order to resolve small changes in amplitude due to the term

$$e^{-kz}\cos(kx)$$

in equation 22.

In the horizontal direction the requirement is that the spacing between nodes is much smaller than the spatial wavelength of the source, i.e.:

$$dx_j << \gamma = 2¶/k \quad \text{for all j} \tag{29}$$

In the vertical direction we must consider the limitations in the layer of air and in the layered earth separately. In the layer of air, the electric field attenuates and reaches the value 1/e when z = 1/k meters. Therefore the nodal spacing must be less than one quarter of that value of z. In the earth the skin depth places a restriction on the vertical nodal spacing. In order to properly account for the skin depth effect, we developed an expression considering the finite nature of the source from equations 8 and 23. This expression is

$$\delta = \frac{1}{(k^4 + (\frac{2\P\mu\sigma}{T})^2)^{1/4} \cos(\tan^{-1}(2\P\mu\sigma/Tk^2)/2)} \tag{30}$$

and reduces to the plane wave skin depth when k = 0.

Plots showing the variation of δ as a function of k for the periods used in MT and MV experiments are shown in Figure 5 for resistivities of 1, 10, 100, and 1 000 ohm-m.

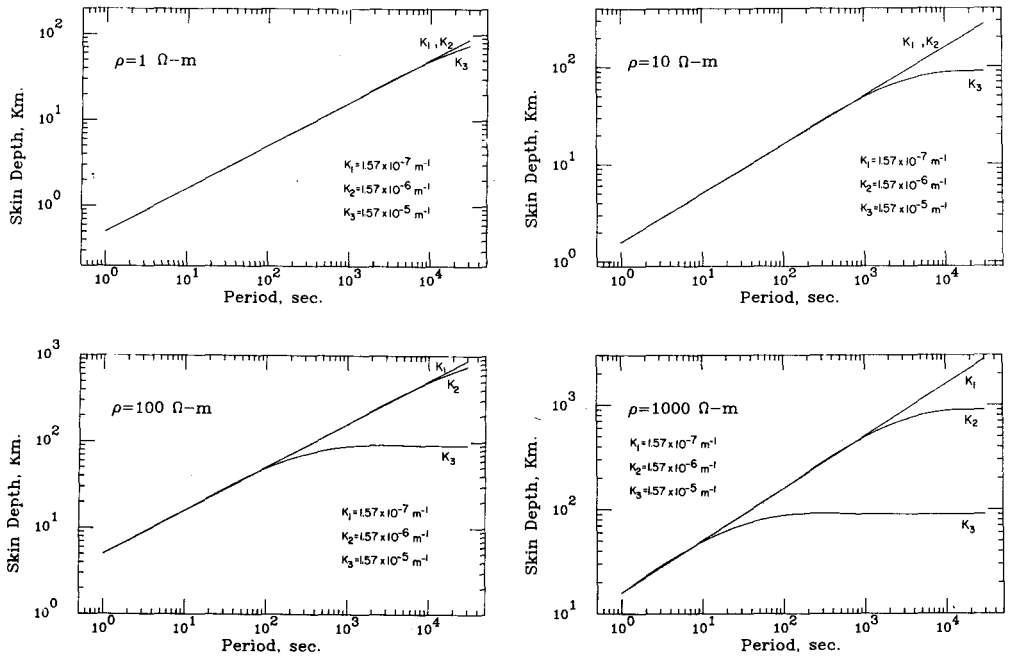

Fig. 5. Skin depth (δ) variation as a function of medium resistivity (ρ), spatial wave number (k) and period (T).

We have plotted the skin depth for three different values of the spatial wave number which according to Price (1962), are in the interval of interest in magnetotelluric investigations. They are $1.57 \times 10^{-7}\,m^{-1}$, $1.57 \times 10^{-6}\,m^{-1}$, and $1.57 \times 10^{-5}\,m^{-1}$.

Although as mentioned before, the general solution to the diffusion equation is obtained by summing all possible solutions over an infinite range of k, we can crudely approximate the line current by a source whose current density has a spatial distribution of the form

$$J = A(1 + \cos(kx)).$$

This can be accomplished by superimposing two simple harmonic sources with spatial wave numbers k_1 and k_2. We set

$$k_1 = k$$

and let k_2 approach to zero (infinite spatial wavelength) by assuming

$$k_2 << k_1.$$

Figure 6 shows the horizontal component of the magnetic field of a line current at a height of 100 km given by equation 16 compared with the approximation A(1+ cos(kx)), when $k = 2\P \times 10^{-6} m^{-1}$ (λ = 1 000 km).

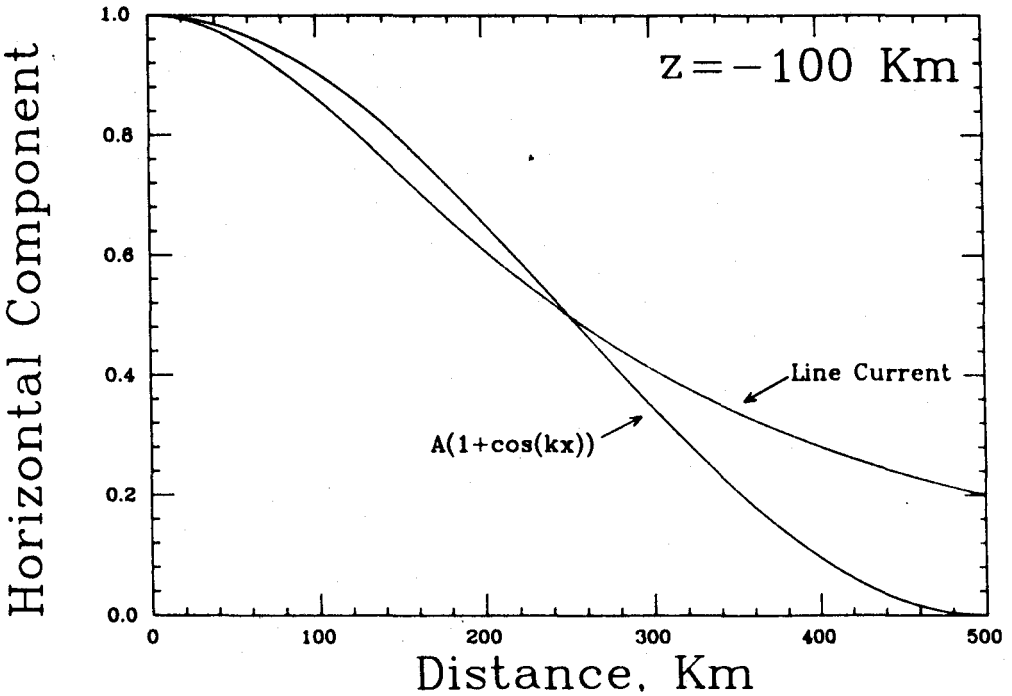

Fig. 6. Horizontal component of the magnetic field due to a line current at a height of 100 km, compared to the approximation A(1+ Cos(kx); $k = 2\pi \times 10^{-6} m^{-1}$ (λ = 1 000 km).

The superposition is performed in our simulation by solving the diffusion equation for each spatial wave number and then adding the corresponding values of the electric field at each node of the grid.

Once the solution to the diffusion equation for the electric field is obtained, equation 3 is used to calculate the horizontal and vertical components of the magnetic field at a particular row of nodes, usually at the surface of the earth. From equation 3 the magnetic field components are given by

$$H_x = -\frac{1}{i\omega\mu}\frac{\partial E_y}{\partial z} \tag{31}$$

and

$$H_z = -\frac{1}{i\omega\mu}\frac{\partial E_y}{\partial x} \tag{32}$$

The derivatives of the electric field are calculated using finite differences. The apparent resistivity as a function of frequency given by the MT method is then given by (Cagniard, 1953, Price, 1962)

$$\rho_{app} = \frac{1}{\omega\mu}\left|\frac{E_y}{H_x}\right|^2 = \frac{1}{\omega\mu}|Z^1|^2 \tag{33}$$

with phase

$$\theta = \tan^{-1}(\mathrm{Im}(Z^1)/\mathrm{Re}(Z^1)) \tag{34}$$

In MV the apparent resistivity is given as a function of frequency, in terms of the complex inductive scale length, $c(\omega)$, introduced by Schmucker (1970) and Kuckes (1973a) by

$$\rho_{app} = \omega\mu|c(\omega)|^2 \tag{35}$$

where

$$c(\omega) = \frac{H_z}{\partial H_x/\partial x} \tag{36}$$

with phase

$$\theta = \tan^{-1}(\mathrm{Im}(c(\omega))/\mathrm{Re}(c(\omega))) \tag{37}$$

NUMERICAL RESULTS

In order to illustrate the application of our numerical algorithm, two models of the Icelandic crust and upper mantle were investigated. This study has been done in order to determine the experimental parameters such as frequency, location of sites,

etc., that minimize the effect of the conducting ocean surrounding the island. The resistivity distribution in these models represents extreme electrical conditions under which electromagnetic soundings would be performed in Iceland.

The models considered represent a north-south cross-section of Iceland as shown in Figure 7. The location of the source is assumed at a height of 110 km above the earth's surface, 250 km to the north of the center of the island, and is oriented such that the current flows in a direction parallel to the strike of the model. All models consist of three layers each. Layer 1 has a resistivity of 0.3 ohm-m and represents the ocean. Its thickness was determined from the bathymetry of Iceland. Immediatly adjacent to the island it is 200 meters thick and 180 km to the north it reaches a thickness of 1 km. To the south the maximum depth of 1 km is reached only 40

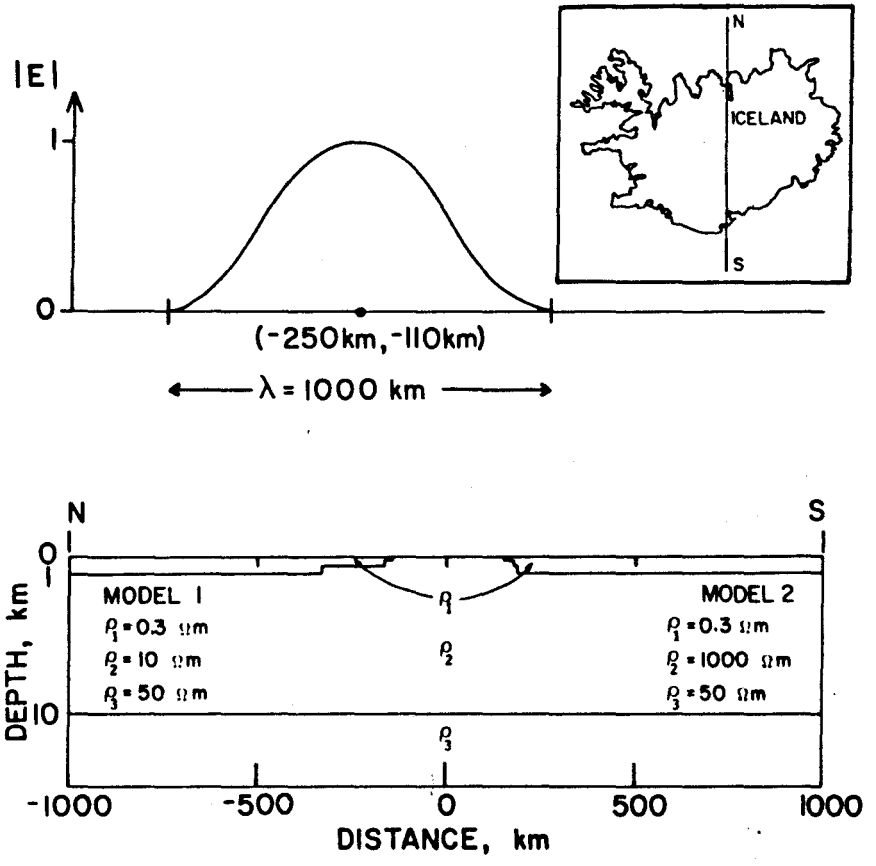

Fig. 7. North-south cross-section of Iceland with the two models considered. The electrojet is located at (-250 km, -110 km). The normalized amplitude of the source electric field is shown as well.

km away from the coast. Layer 2 has a resistivity of 10 ohm-m in model 1 and a resistivity of 1 000 ohm-m in model 2. According to Björnsson (1976) and Thayer *et al.* (1981), these two values can be considered as representative of the two extremes found for the resistivity of the Icelandic crust. This layer extends to a depth of 10 km and is underlain by a third layer having a resistivity of 50 ohm-m which represents the upper mantle beneath Iceland.

The simulation was performed at three different periods of 30, 300, and 3 000 seconds. In Figures 8 and 9 we show the absolute value of vertical and horizontal components of the magnetic field, as well as the electric field, at the surface of the model as a function of position for the two models under study, and for the three periods considered. These plots have been made in arbitrary units keeping the relative amplitudes of the fields constant. We have also plotted these three fields for the cases in which the ocean has been removed from the models considered and we have only the two layer structure. It is important to recognize the difference between the two models as far as the effect of the interfaces is less pronounced as in the case of model 2 (Figure 9), where the resistivity of the crust is 1 000 ohm-m. This is due to the fact that in model 1 the difference in magnitude between the induced currents on both sides of the ocean-land interface, is less than in the case of model 2. This, in turn, is due to the contrast in resistivity. The greater the resistivity of the medium, the smaller the magnitude of the induced currents. For the horizontal component this results in an attenuation of the field over the material with larger resistivity. The vertical component at the interface increases a great deal because the induced currents in the ocean produce a much larger vertical magnetic field than the currents induced inland. These can be noticed when comparing the vertical fields for the three periods in the two different models. Model 1 has a smaller vertical component than Model 2 at the interface at all three periods. Of course the larger the resistivity the larger the magnitude of the electric field.

As we shall see in what follows, these effects combined give place to a substantial difference between the apparent resistivity given by the magnetotelluric method (equation 33) and the apparent resistivity given by the magnetic variation method (equation 35). It is also important to note that the effect in the vertical magnetic field increases with increasing period whereas for the horizontal magnetic field as well as on the electric field, the longer the period, the less pronounced the effect. This may occur because the anomalous vertical magnetic field is a local effect of the interface whereas the horizontal magnetic and electric fields carry the characteristics of a broader induction process.

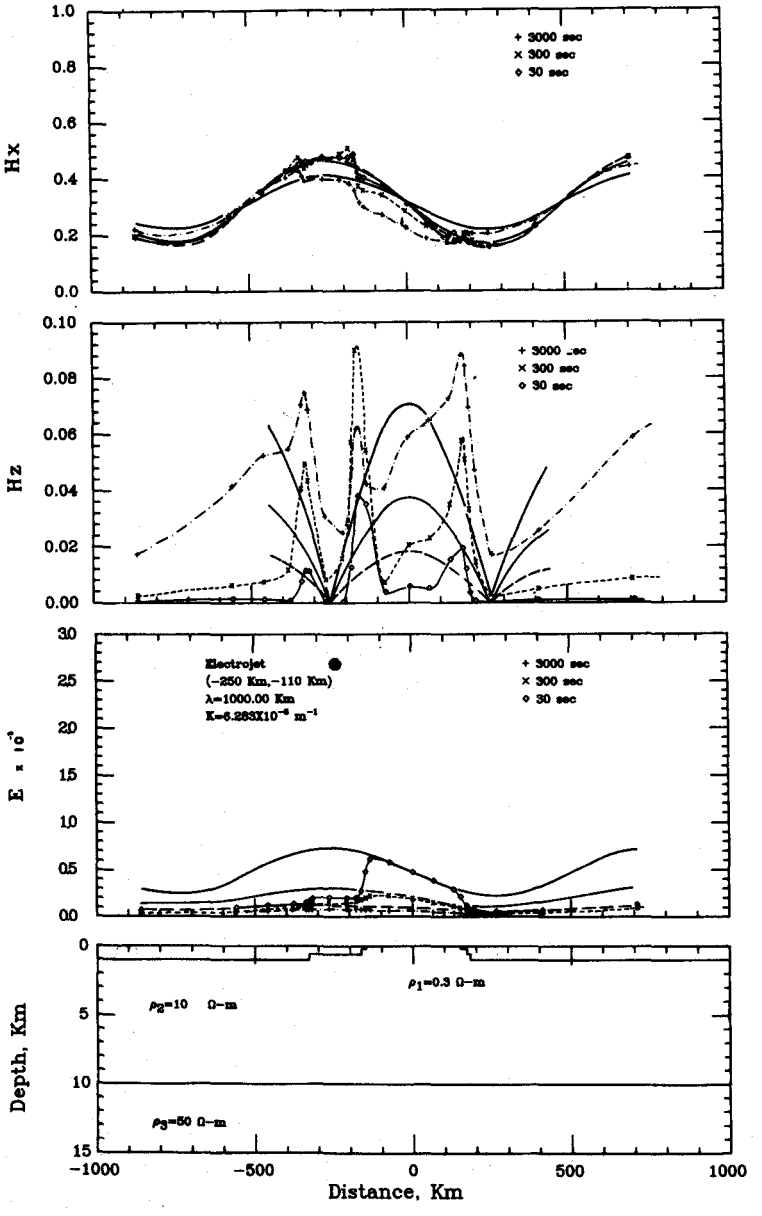

Fig. 8. Model 1. Electric and magnetic fields behaviour. Dashed lines →T = 3 000 sec.; thin solid lines →300 sec; heavy solid lines →30 sec. Lines correspond to the response without the ocean. Symbols correspond to the response of the model with the ocean.

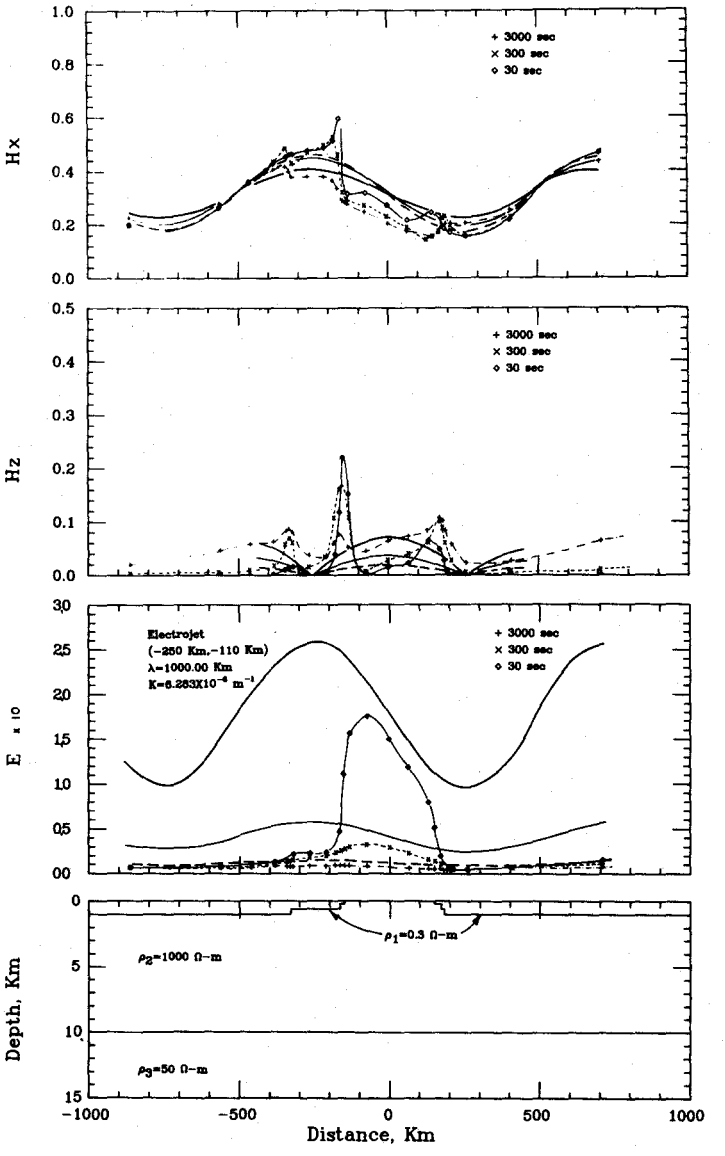

Fig. 9. Model 2 (ρ_{crust} = 1 000 Ω-m). Fields response with and without the ocean. For key see Figure 8.

In Figures 10 and 11 we show the apparent resistivity as a function of position as given by the MT and MV methods. In Figure 10 the responses of model 1 (ρ(crust) = 10 ohm-m) for the three periods considered are shown whereas in Figure 11 we show the correponding responses for model 2 (ρ(crust) = 1 000 ohm-m). In these figures we have also plotted, as continuous lines, the apparent resistivity for both methods as given by the two layer model which results when the ocean is removed from the structure shown. It is interesting to note that in this case the responses given by the two methods are essentially the same, this fact has been pointed out from a theoretical standpoint by Schmucker (1970) and Kuckes (1973b). With increasing period the MT and MV responses depart from each other at the extremes of the model, this departure is caused by the lack of accuracy at the extremes of the nodal mesh. Since the number of nodes in each direction is limited to 25, the shape of the fields is not well resolved where there are a few nodes and their spacing is large. Due to the limited number of nodes available we have concentrated most of them in the center of the island and around the ocean-land interfaces.

From Figures 10 and 11 it can be seen how the period at which the measurements are made and the resistivity contrast at the ocean-land interface determine the importance of the ocean effect in magnetic soundings. For long periods and a large contrast in resistivity, the situation represented in Figure 11, the edge effect is detected across the entire island. Only at positions around its center, does the apparent resistivity determined by the magnetic fields alone, coincide with that determined by the magnetotelluric method. This is due to the fact that the vertical component of the magnetic field is much more affected by the ocean edge effect than is the horizontal magnetic field component or the electric field component. This can be seen in Figures 8 and 9. As the period decreases, the effect of the ocean becomes less important in the interior of the island. However, when the crustal resistivity is large, as is the case of model 2, the effect of the ocean is still important. This is a consequence of the way in which the skin depth varies as a function of period for a given resistivity. When the resistivity is large for the spatial wave number considered, the difference between the skin depth at 3 000 seconds and at 30 seconds is only about 50 km, whereas when the resistivity is small, as is the case of model 1, this difference is about 100 km. This is why the ocean effect is detected at distances from the coast comparable with the skin depth.

We conclude that for locations within one skin depth from the ocean-land interface, the apparent resistivity measured with the magnetic variation method is perturbed very strongly by the presence of the conducting ocean. In our modelling this

effect is enhanced because we have determined the nodal spacings as a function of the computer limitations such as storage, etc. The separation between nodes in the horizontal direction may be too coarse to accurately calculate gradients of the electric field and the horizontal component of the magnetic field. It would be possible to determine with more accuracy the region in the vicinity of the coast which is

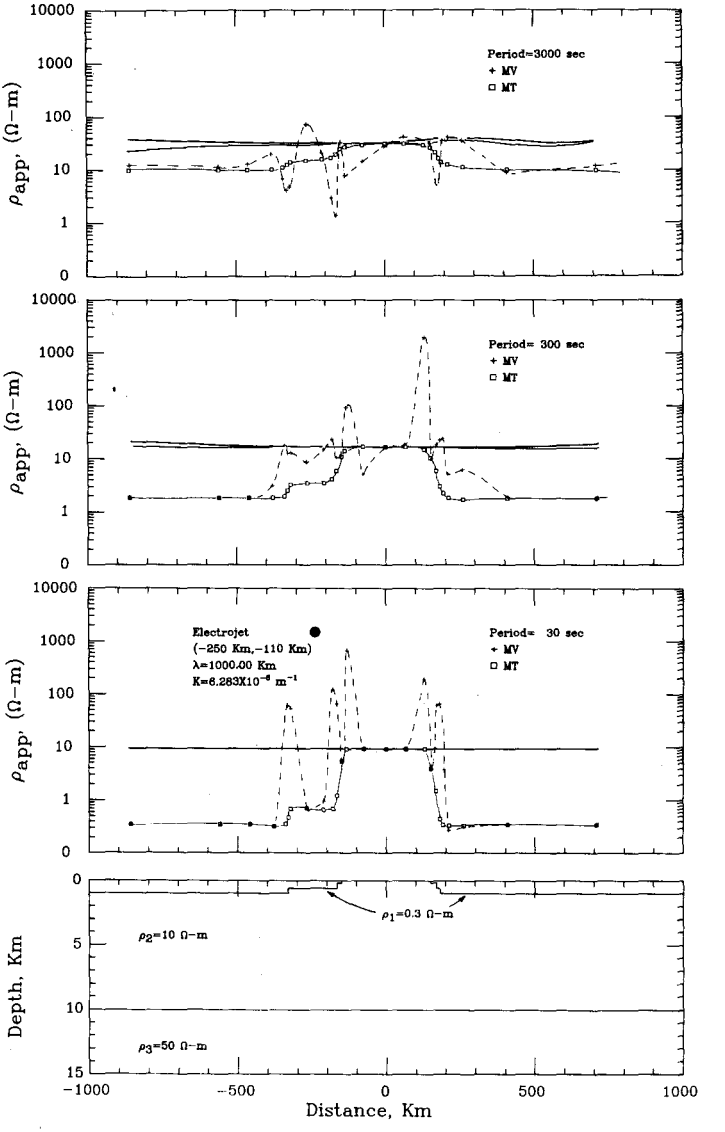

Fig. 10. Model 1 (ρ_{crust} = 10 Ω-m). Apparent resistivity response for MV and MT methods given by the finite difference algorithm. Solid lines correspond to the homogeneous two-layer model without the ocean.

affected by the interface if we had the possibility of using more nodes in the grid. Also we must keep in mind the limitations on this approach regarding its two dimensionality. This implies an infinite structure in the direction of the strike and in a real situation the surrounding ocean may produce three dimensional effects that we are not accounting for.

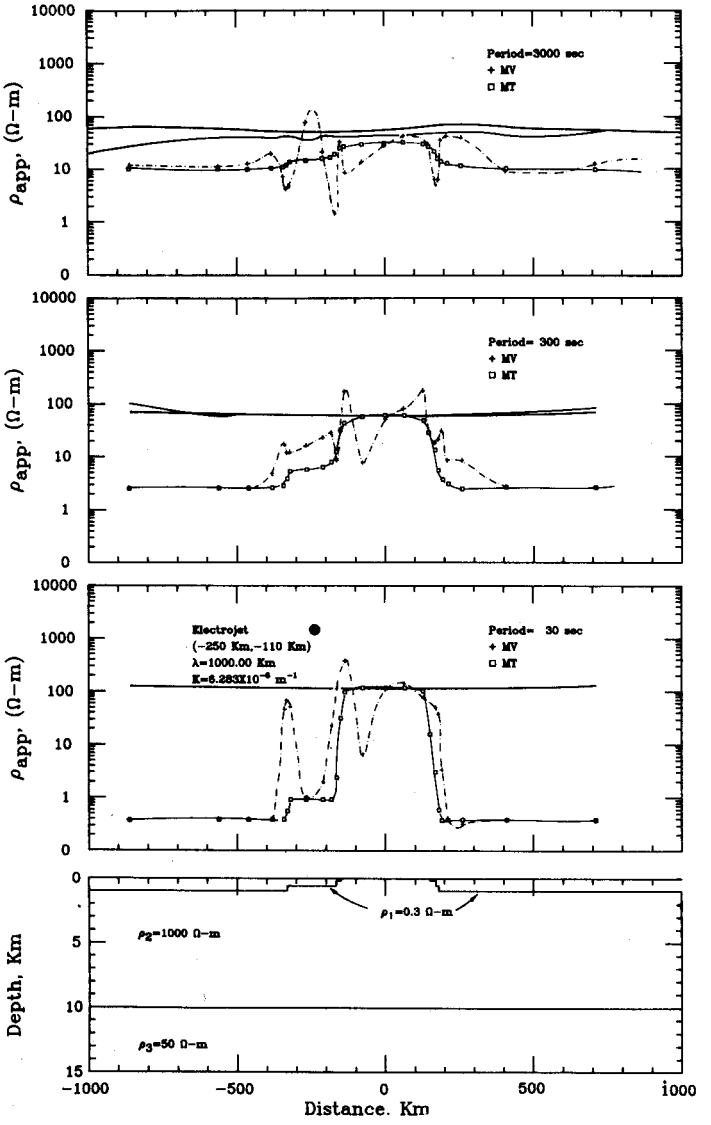

Fig. 11. Model 2 (ρ_{crust} = 1 000 Ω-m). Apparent resistivity responses for MV and MT methods given by the finite difference algorithm. Solid lines correspond to the homogeneous two-layer model without the ocean.

CONCLUSIONS

We have outlined a somewhat general algorithm for finite difference simulation of the electromagnetic induction due to a finite spatial wavelength driving source field. We applied this algorithm for the problem of induction in a homogeneous stratified earth with embedded inhomogeneities in resistivity. The accuracy of the solution depends strongly on the generation of boundary conditions and on the choice of mesh size. We considered the case in which the electrojet is a superposition of two simple harmonic sources and is parallel to the strike of the geoelectric inhomogeneities. More work has to be done in order to solve the problem of simulating the induction due to a source perpendicular to the strike.

Two models representing possible characteristics of the Icelandic crust and upper mantle were investigated in order to give some insight into the effects of the conducting ocean on magnetic and magnetotelluric soundings in Iceland.

It should be pointed out that the above results are approximate and qualitative to some extent.

ACKNOWLEDGMENTS

The author wishes to thank Professor John F. Hermance for his useful remarks. The computer time was provided by the Department of Geological Sciences of Brown University.

BIBLIOGRAPHY

BJÖRNSSON, A., 1976. Electrical resistivity of layer 3 in the Icelandic crust, *Visindafelag Islendiga* (Science Society of Iceland), Greinar, *V*, 1-22.

BREWITT-TAYLOR, C. R. and J. T. WEAVER, 1976. On the finite difference solution of two dimensional induction problems. *Geophys. J. R. Astr. Soc., 47,* 375-396.

CAGNIARD, L., 1953. Basic theory of the magnetotelluric method of geophysical prospecting, *Geophysics,* 18, 605-635.

HERMANCE, J. F., 1976. General templates for finite difference simulation of two-dimensional electrical inhomogeneities. *Internal Report* Geophysical Laboratory, Department of Geological Sciences, Brown University.

HERMANCE, J. F., 1978. Electromagnetic induction in the earth by moving ionospheric current systems, *Geophys. J. R. Astr. Soc., 55,* 557-576.

HIBBS, R. D. and F. W. JONES, 1973 Electromagnetic induction in the earth by a non-symmetric non-uniform source. *J. Geomag. Geoelectr., 25,* 75-86.

JONES, F. W. and L. J. PASCOE, 1971. A general computer program to determine the perturbation of alternating electric currents in a two dimensional model of a region of uniform conductivity with an embedded inhomogeneity. *Geophys. J. R. Astr. Soc., 23,* 3-30.

KUCKES, A. F., 1973a. Relations between electrical conductivity of a mantle and fluctuating magnetic fields. *Geophys. J. Roy. Astron. Soc., 32,* 119-131.

KUCKES, A. F., 1973b. Correspondence between the magnetotelluric and field perturbation depth analyses for measuring electrical conductivity. *Geophys. J. R. Astr. Soc.,* 32, 381-385.

PRAUS, O., 1976. Numerical solutions of the MT field in inhomogeneous structures, *Geoelectric and Geothermal Studies* (East-Central Europe, Soviet Asia) KAPG Geophysical Monograph. Akademiai Kiado, Budapest.

PRICE, A. T., 1962. The theory of magnetotelluric methods when the source field is considered. *J. Geophys. Res., 67,* 5, 1907-1918.

RAMO, S., J. R. WHINNERY and T. VAN DUZER, 1965. Fields and waves in communication electronics. John Wiley and Sons, Inc., New York, NY.

SCHMUCKER, U., 1970. Anomalies of geomagnetic variations in the south western United States. *Bull. Scripps Inst. Oceanogr.,* 13.

THAYER, R. E., A. BJÖRNSSON, L. ALVAREZ and J. F. HERMANCE, 1981. Magma genesis and crustal spreading in the northern neovolcanic zone of Iceland: Telluric-magnetotelluric constraints. *Geophys. J. R. Astr. Soc.,* 65, 423-442.

WILLIAMSON, K., C. HEWLETT and Y. TAMMEMAGI, 1974. Computer modelling of electrical conductivity structures. *Geophys. J. R. Astr. Soc., 37,* 533-536.